INTERNATIONAL JOURNAL FOR NUMERICAL METHODS IN FLUIDS
Int. J. Numer. Meth. Fluids 2007; **55**:1157–1169
Published online 3 May 2007 in Wiley InterScience (www.interscience.wiley.com). DOI: 10.1002/fld.1511

Viscous dissipative fluid flow past a semi-infinite vertical plate with variable surface temperature

G. Palani*, †

Department of Applied Mathematics, Sri Venkateswara College of Engineering, Pennalur, Sriperumbudur, Kancheepuram District 602 105, Tamil Nadu, India

SUMMARY

An analysis of the effect of viscous dissipative heat on two-dimensional viscous incompressible fluid flow past a semi-infinite vertical plate with variable surface temperature is carried out. The dimensionless governing equations are unsteady, two-dimensional, coupled, and non-linear governing equations. A most accurate, unconditionally stable and fast converging implicit finite-difference scheme is used to solve the non-dimensional governing equations. Velocity and temperature of the flow have been presented graphically for various parameters occurring in the problem. The local and average skin friction and Nusselt number are also shown graphically. It is observed that greater viscous dissipative heat causes a rise in the temperature. Copyright © 2007 John Wiley & Sons, Ltd.

Received 4 April 2006; Revised 13 December 2006; Accepted 12 March 2007

INTRODUCTION

Hear transfer by natural convection is frequently encountered in our environment and engineering devices. Two-dimensional free convection flows past a semi-infinite plate have received the attention of many researchers because of their wide applications in industry and technological fields. Polhausen [1] and Ostrich [2] studied steady free convective flow past a semi-infinite vertical plate by integral and similarity methods, respectively. Hellums and Churchill [3] first studied transient free convective flow past a semi-infinite vertical plate by explicit finite-difference method. Soundalgekar and Ganesan [4] studied the problem of transient free convective flow of an incompressible viscous fluid past a semi-infinite isothermal vertical plate by an implicit finite-difference method, which is unconditionally stable. In all these papers, the viscous dissipative heat was neglected. However, Gebhart [5] studied the importance of viscous dissipative heat in free convection flows on a vertical surface subject to isothermal and uniform-flux surface conditions.

*Correspondence to: G. Palani, Department of Applied Mathematics, Sri Venkateswara College of Engineering, Pennalur, Sriperumbudur, Kancheepuram District 602 105, Tamil Nadu, India.
†E-mail: gpalani32@yahoo.co.in, palani@svce.ac.in

Soundalgekar *et al*. [6] also studied the transient free convection flows of viscous dissipative fluid past a semi-infinite isothermal vertical plate by using an implicit finite-difference scheme. Ganesan and Palani [7] studied free convective viscous dissipative fluid flow past a semi-infinite inclined plate by using an implicit finite-difference scheme. Capper *et al*. [8] studied formulae for second-order two-point, boundary value problems. Obrenchkoff-type formulas for finding y_n are derived and these methods are of sixth- and eighth-order accuracy. Variable-step Runge–Kutta Nystrom methods for the numerical solution of reversible systems were studied by Cash and Girdlestone [9]. The problem of implementing reversible Runge–Kutta Nystrom reversible integration formulae with varying steps was studied in detail. Discrete conservative vector fields induced by the trapezoidal method were studied by Iavernaro and Trigiante [10]. BS linear multistep methods on non-uniform meshes were studied by Mazzia *et al*. [11].

Viscous dissipation occurs in natural convection in natural devices. Such dissipation effects may also be present in stronger gravitational fields and in processes wherein the scale of the process is very large, e.g. on larger planets, in large masses of gas in space and in geological processes in fluids internal to various bodies. The heat due to viscous dissipation in the energy equation is very small and is neglected. However, when the gravitational force is intensive or when the Prandtl number of the fluid is very high, the viscous dissipative effects cannot be neglected.

However, the effect of viscous dissipation in the transient free convection flow of a viscous incompressible fluid past a semi-infinite vertical plate with variable surface temperature has not been studied. Hence, the present attempt is to solve the problem of the transient free convection flow of viscous incompressible fluid past a semi-infinite vertical plate with variable surface temperature by taking into consideration the viscous dissipative heat and solving the governing non-linear equations by using the implicit finite-difference scheme of Crank–Nicholson type and studying the effects of viscous dissipative heat on the time to reach the steady state.

MATHEMATICAL FORMULATION

A two-dimensional unsteady viscous incompressible fluid flow past a semi-infinite vertical plate with variable surface temperature is assumed. Initially, at time $t' \leqslant 0$, it is assumed that the plate and the fluid are at the same temperature and at time $t' > 0$, the temperature of the plate is suddenly raised to $T'_w(x) = T'_\infty + ax^n$ causing currents to flow in the vicinity of the plate. The x-axis is measured along the plate and y-axis is taken along upward normal to the plate. The effect of viscous dissipation in the energy equation is considered. Then under these assumptions, the governing boundary layer equations of mass, momentum and energy for free convection flows with Boussinesq's approximation are as follows:

$$\frac{\partial u}{\partial x} + \frac{\partial v}{\partial y} = 0 \tag{1}$$

$$\frac{\partial u}{\partial t'} + u\frac{\partial u}{\partial x} + v\frac{\partial u}{\partial y} = g\beta(T' - T'_\infty) + \nu\frac{\partial^2 u}{\partial y^2} \tag{2}$$

$$\frac{\partial T'}{\partial t'} + u\frac{\partial T'}{\partial x} + v\frac{\partial T'}{\partial y} = \alpha\frac{\partial^2 T'}{\partial y^2} + \frac{\mu}{\rho C_p}\left(\frac{\partial u}{\partial y}\right)^2 \tag{3}$$

DOI: 10.1002/fld

The initial and boundary conditions are

$$\begin{aligned} t' \leqslant 0:\ & u = 0, \quad v = 0, \quad T' = T'_\infty \\ t' > 0:\ & u = 0, \quad v = 0, \quad T'_{\mathrm{w}}(x) = T'_\infty + ax^n \quad \text{at } y = 0 \\ & u = 0, \quad T' = T'_\infty, \quad \text{at } x = 0 \\ & u \to 0, \quad T' \to T'_\infty, \quad \text{as } y \to \infty \end{aligned} \tag{4}$$

Introducing the following non-dimensional quantities:

$$\begin{aligned} & X = \frac{x}{L}, \quad Y = \frac{y}{L} Gr^{1/4}, \quad U = \frac{uL}{v} Gr^{-1/2} \\ & V = \frac{vL}{v} Gr^{-1/4}, \quad t = \frac{vt'}{L^2} Gr^{1/2}, \quad T = \frac{T' - T'_\infty}{T'_{\mathrm{w}}(L) - T'_\infty} \\ & Gr = \frac{g\beta L^3 (T'_{\mathrm{w}}(L) - T'_\infty)}{\upsilon^2}, \quad Pr = \frac{v}{\alpha} \end{aligned} \tag{5}$$

Equations (1)–(4) are reduced to the following non-dimensional form:

$$\frac{\partial U}{\partial X} + \frac{\partial V}{\partial Y} = 0 \tag{6}$$

$$\frac{\partial U}{\partial t} + U \frac{\partial U}{\partial X} + V \frac{\partial U}{\partial Y} = T + \frac{\partial^2 U}{\partial Y^2} \tag{7}$$

$$\frac{\partial T}{\partial t} + U \frac{\partial T}{\partial X} + V \frac{\partial T}{\partial Y} = \frac{1}{Pr} \frac{\partial^2 T}{\partial Y^2} + \varepsilon \left(\frac{\partial U}{\partial Y} \right)^2 \tag{8}$$

where $\varepsilon = g\beta L / C_p$.

Here ε is the dissipation number, which is equal to the ratio of the kinetic energy of the flow and the heat, transferred to the fluid.

The corresponding initial and boundary conditions in non-dimensional quantities are given by

$$\begin{aligned} t \leqslant 0:\ & U = 0, \quad V = 0, \quad T = 0 \\ t > 0:\ & U = 0, \quad V = 0, \quad T = X^n \quad \text{at } Y = 0 \\ & U = 0, \quad T = 0 \quad \text{at } X = 0 \\ & U \to 0, \quad T \to 0 \quad \text{as } Y \to \infty \end{aligned} \tag{9}$$

NUMERICAL PROCEDURE

The two-dimensional, non-linear, unsteady, and coupled partial differential equations (6)–(8) under the initial and boundary conditions (9) are solved using an implicit finite-difference scheme of Crank–Nicolson type which is fast convergent and unconditionally stable.

DOI: 10.1002/fld

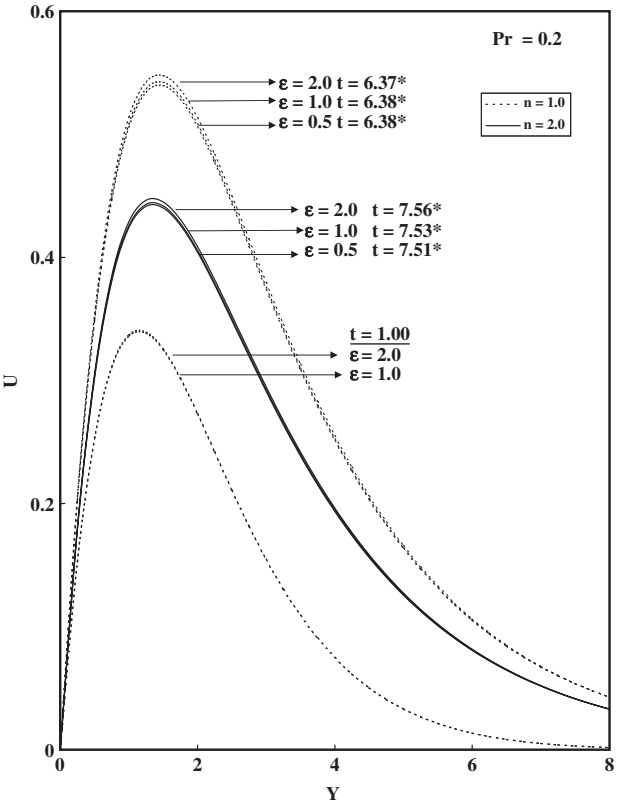

Figure 1. Transient velocity profiles at $X = 1.0$ for different n and ε ($*$ steady state).

The finite-difference equation corresponding to Equations (6)–(8) are given by

$$\frac{U_{i,j-1}^{k+1} - U_{i-1,j-1}^{k+1} + U_{i,j}^{k+1} - U_{i-1,j}^{k+1} + U_{i,j-1}^{k} - U_{i-1,j-1}^{k} + U_{i,j}^{k} - U_{i-1,j}^{k}}{4\Delta X} + \frac{V_{i,j}^{k+1} - V_{i,j-1}^{k+1} + V_{i,j}^{k} - V_{i,j-1}^{k}}{2\Delta Y} = 0 \tag{10}$$

$$\frac{U_{i,j}^{k+1} - U_{i,j}^{k}}{\Delta t} + U_{i,j}^{k} \frac{(U_{i,j}^{k+1} - U_{i-1,j}^{k+1} + U_{i,j}^{k} - U_{i-1,j}^{k})}{2\Delta X} + V_{i,j}^{k} \frac{(U_{i,j+1}^{k+1} - U_{i,j-1}^{k+1} + U_{i,j+1}^{k} - U_{i,j-1}^{k})}{4\Delta Y} = \frac{[T_{i,j}^{k+1} + T_{i,j}^{k}]}{2} + \frac{(U_{i,j-1}^{k+1} - 2U_{i,j}^{k+1} + U_{i,j+1}^{k+1} + U_{i,j-1}^{k} - 2U_{i,j}^{k} + U_{i,j+1}^{k})}{2(\Delta Y)^2} \tag{11}$$

DOI: 10.1002/fld

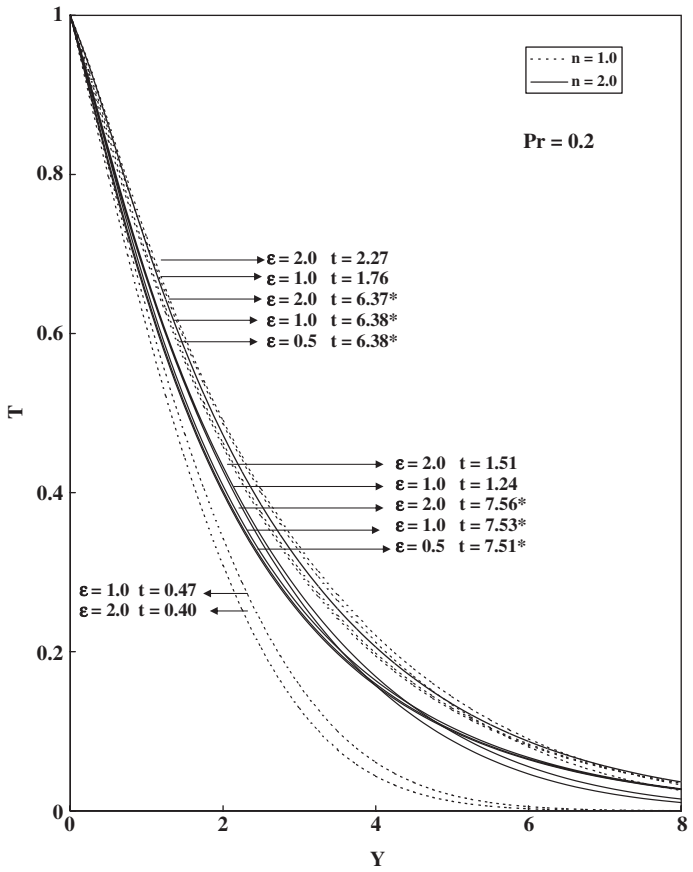

Figure 2. Transient temperature profiles at $X = 1$ for different n and ε ($*$ steady state).

$$\frac{T_{i,j}^{k+1} - T_{i,j}^{k}}{\Delta t} + U_{i,j}^{k} \frac{(T_{i,j}^{k+1} - T_{i-1,j}^{k+1} + T_{i,j}^{k} - T_{i-1,j}^{k})}{2\Delta X} + V_{i,j}^{k} \frac{(T_{i,j+1}^{k+1} - T_{i,j-1}^{k+1} + T_{i,j+1}^{k} - T_{i,j-1}^{k})}{4\Delta Y} = \frac{(T_{i,j-1}^{k+1} - 2T_{i,j}^{k+1} + T_{i,j+1}^{k+1} + T_{i,j-1}^{k} - 2T_{i,j}^{k} + T_{i,j+1}^{k})}{2\,Pr(\Delta Y)^2} + \varepsilon \left[\frac{(U_{i,j+1}^{k+1} - U_{i,j-1}^{k+1} + U_{i,j+1}^{k} - U_{i,j-1}^{k})}{4\Delta Y} \right]^2 \tag{12}$$

DOI: 10.1002/fld

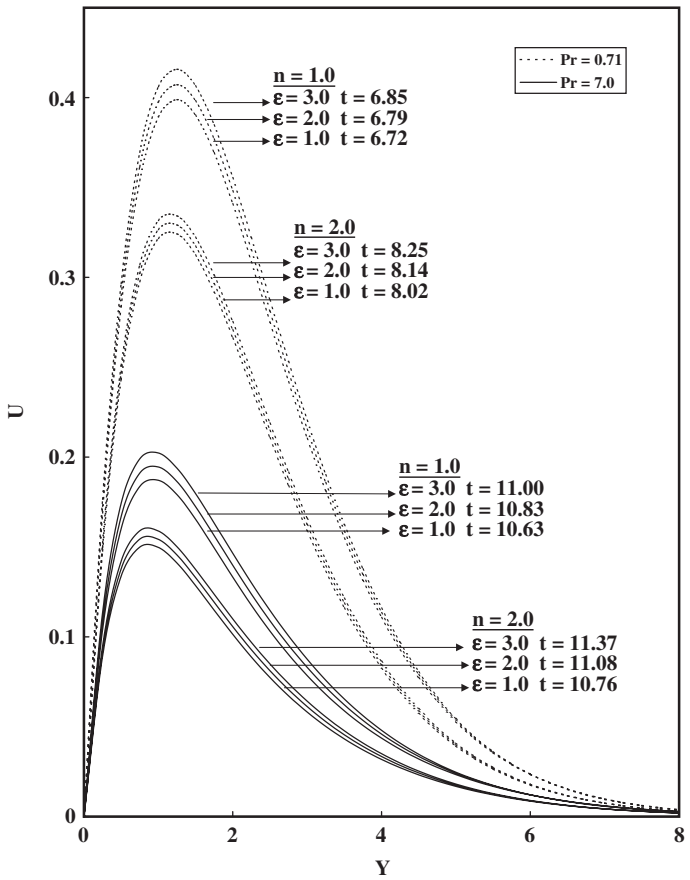

Figure 3. Steady-state velocity profiles at $X = 1.0$ for different Pr, n and ε.

The values of U, V and T are known at all grid points at $t = 0$ from the initial conditions. During any one time step, $U_{i,j}^k$ and $V_{i,j}^k$ appearing in the finite-difference equation are treated as constants. The U, V and T are calculated at $(k+1)$th time level using the known values at previous kth time level and this can be done as follows.

Equation (12) at every internal nodal point on a particular i level constitutes a tri-diagonal system of equations, which are solved by Thomas algorithm, described by Carnahan *et al.* [12]. Thus, the values of T are found at every nodal point on a particular i at $(k+1)$th time level. Using the values of T at $(k+1)$th time level in Equation (11), the values of U at $(k+1)$th time level are found in a similar manner. Then, the values of V are calculated explicitly by using Equation (10) at every nodal point on a particular i level. This process is repeated for various i levels. Thus, the values of T, U and V are known at all grid points in the rectangular region at $(k+1)$th time level.

This process is repeated in time until steady state is reached. The steady-state solution is assumed to have been reached, when the absolute differences between values of U as well as temperature T at two consecutive time steps are less than 10^{-5} at all grid points. Computations have been carried out for different values of parameters.

DOI: 10.1002/fld

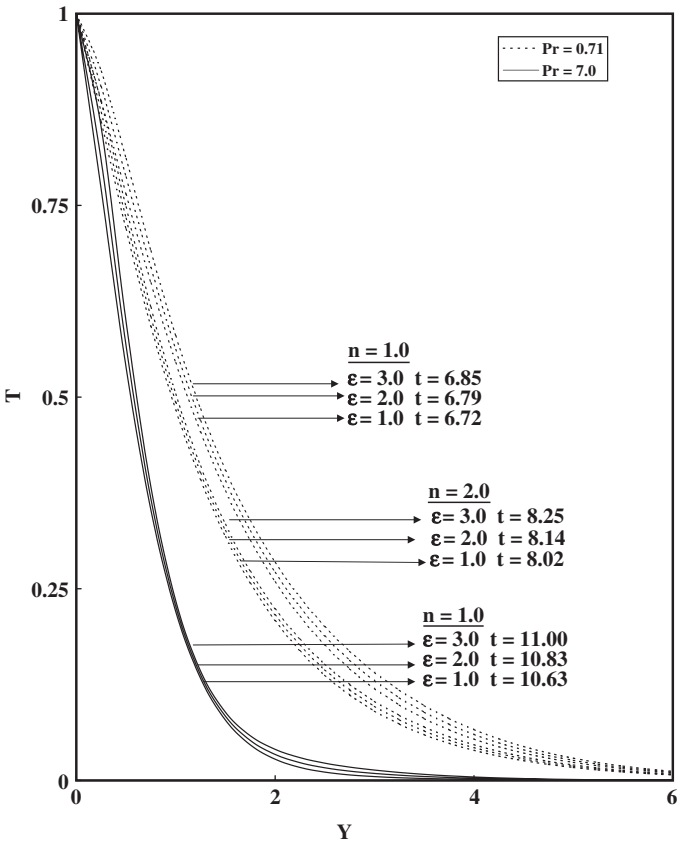

Figure 4. Steady-state temperature profiles at $X = 1.0$ for different Pr, n and ε.

The region of integration is considered as a rectangle with sides $X_{\max}(= 1.0)$ and $Y_{\max}$ $(= 24.0)$ where $Y_{\max}$ corresponds to $Y = \infty$ which lies very well outside the momentum and thermal boundary layers. After experimenting with a few sets of mesh sizes, the mesh sizes are fixed as $\Delta X = 0.05$, $\Delta Y = 0.25$ and $\Delta t = 0.01$. The Crank–Nicolson implicit finite-difference scheme is always stable and convergent.

RESULTS AND DISCUSSION

We have computed the time required to reach the steady state for different values of the dissipation parameter ε, for fluids with the Prandtl number and exponent n, power law for variable surface temperature. In Figures 1 and 2, the transient velocity and temperature profiles are shown for n and dissipation parameter ε. Velocity increases steadily as time advances, reaching steady state. When n increases, the temperature gradient along the plate near the leading edge decreases. That is, the impulsive force along the plate decreases with increasing n. Due to these facts, the difference between the temporal maximum value and steady-state value decreases with n. Both velocity and temperature decrease as n increases.

DOI: 10.1002/fld

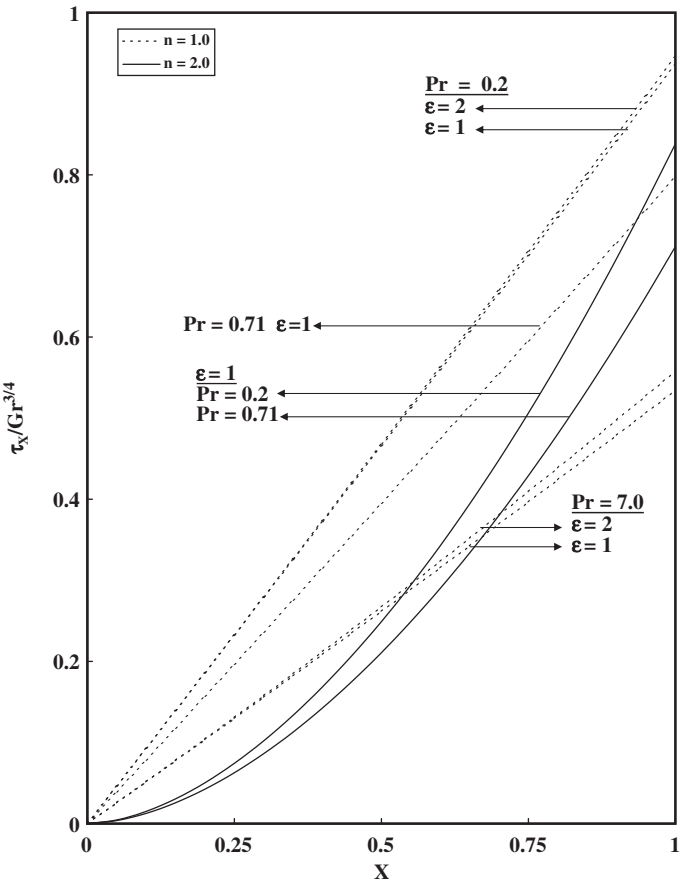

Figure 5. Local skin friction.

In Figures 3 and 4, the steady-state velocity and temperature profile at $X = 1.0$ for different Pr, n and ε are shown. We observe from these curves that steady-state velocity increases with greater viscous dissipative heat for all Prandtl number of the fluids. From both these figures, we observe that the steady-state velocity decreases with an increasing Prandtl number. However, the time required to reach steady state increases with the increasing Prandtl number of the fluid. It is observed that the temperature increases with a greater viscous dissipative heat irrespective of the Prandtl number of the fluid. Also, we observed from these figures that temperature decreases as Pr increases.

Knowing the velocity and temperature field, it is interesting to study from the practical point of view, the skin friction and the rate of heat transfer. The local and average skin friction and Nusselt number, in non-dimensional quantities are

$$\tau_X = Gr^{3/4} \left(\frac{\partial U}{\partial Y} \right)_{Y=0} \tag{13}$$

DOI: 10.1002/fld

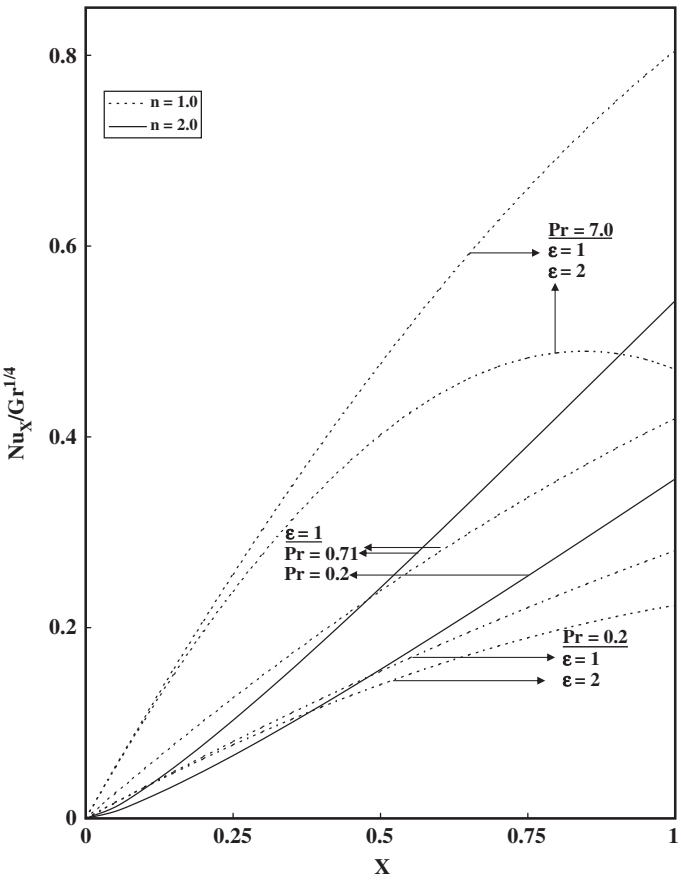

Figure 6. Local Nusselt number.

$$\overline{\tau} = Gr^{3/4} \int_0^1 \left[\frac{\partial U}{\partial Y}\right]_{Y=0} \mathrm{d}X \tag{14}$$

$$Nu_X = -X\, Gr^{1/4} \left(\frac{\partial T}{\partial Y}\right)_{Y=0} \Big/ T_{Y=0} \tag{15}$$

$$\overline{Nu} = -Gr^{1/4} \int_0^1 \left[\left(\frac{\partial T}{\partial Y}\right)_{Y=0} \Big/ T_{Y=0}\right] \mathrm{d}X \tag{16}$$

The derivatives involved in Equations (13)–(16) are evaluated by using a five-point approximation formula and then the integrals are evaluated by Newton–Cotes-closed integration formula.

The local wall shear stress decreases as Pr increases, because velocity decreases with an increasing value of Pr. Also, it is observed that local skin friction decreases as n increases (Figure 5). This is because of the fact that the velocity gradient decreases near the plate as n increases which is shown in Figure 3. Greater viscous dissipative heat causes a rise in the local skin friction.

DOI: 10.1002/fld

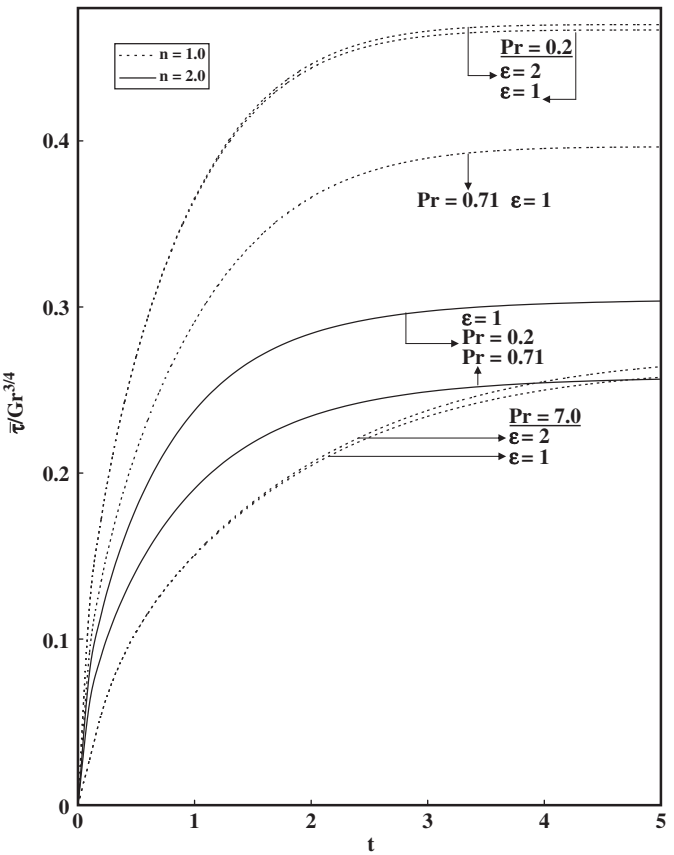

Figure 7. Average skin friction.

Local Nusselt number is shown in Figure 6 and it is observed that Nusselt number increases with n. However, it is observed that the above trend is reversed near the leading edge. The local Nusselt number increases with Pr. Also, it is observed that greater viscous dissipative heat causes a decrease in the local Nusselt number.

Average skin friction and Nusselt number are plotted in Figures 7 and 8, respectively. Average skin friction decreases as n increases. This is due to the fact that the velocity gradient near the plate decreases as n increases. The average skin friction increases with time 't' and then remains stationary for large values of 't'. A greater viscous dissipative heat causes a rise in the average skin friction. Average skin friction decreases with increasing Pr throughout the transient period.

Figure 8 shows that there is no change in average Nusselt number in the initial period with respect to n. This reveals that initially heat transfer is due to conduction only. In the initial convection period average Nusselt number decreases slightly and then increases with n. Also, we observed from these figures that the average Nusselt number decreases with an increase of the viscous dissipation parameter irrespective of the Prandtl number. The average Nusselt number increases with increasing Pr.

DOI: 10.1002/fld

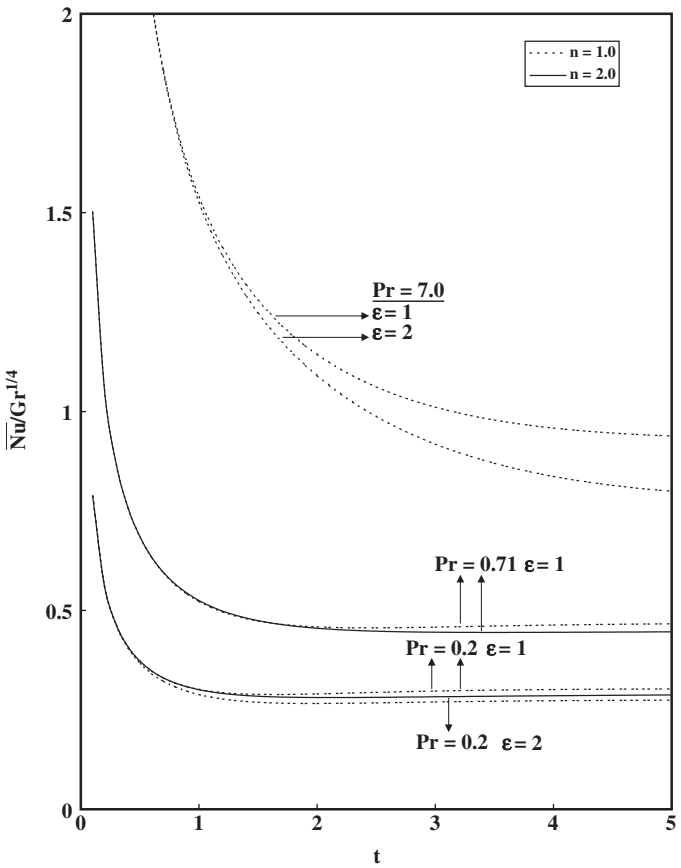

Figure 8. Average Nusselt number.

NOMENCLATURE

a	constant
C_p	constant pressure specific heat
Gr	Grashof number
g	acceleration due to gravity
L	reference length
n	exponent in the power law variation of the wall temperature
$\overline{Nu}$	dimensionless average Nusselt number
Nu_X	dimensionless local Nusselt number
Pr	Prandtl number
T'	temperature
T	dimensionless temperature
t'	time

DOI: 10.1002/fld

t	dimensionless time
u, v	velocity components in x, y directions, respectively
U, V	dimensionless velocity components in X, Y directions, respectively
x	spatial coordinate along the plate
X	dimensionless spatial coordinate
y	spatial coordinate along upward normal to the plate
Y	dimensionless spatial coordinate along upward normal to the plate

Greek symbols

α	thermal diffusivity
β	volumetric coefficient of thermal expansion
ε	dissipation number
μ	coefficient of viscosity
ν	kinematic viscosity
ρ	density
τ_X	dimensionless local skin friction
$\overline{\tau}$	dimensionless average skin friction

Subscripts

i	grid point along the X direction
j	grid point along the Y direction
w	conditions on the wall
∞	free stream condition

Superscript

k	time step level

REFERENCES

1. Pohlhausen E. Der Wärneaustausch zwischen festen Körpern und Flüssigkeiten mit Kleiner Reibung und Kleiner Wärmeleitung. *ZAMM* 1921; **1**:115–121.
2. Ostrich S. *NACA Report*, vol. 1111, 1953; 63.
3. Hellums JD, Churchill SW. Transient and steady state, free and natural convection, numerical solutions: Part 1. The isothermal vertical plate. *AIChE Journal* 1962; **8**:690–692.
4. Soundalgekar VM, Ganesan P. Finite difference analysis of transient free convection on an isothermal vertical flat plate. *Regional Journal of Energy Heat Mass Transfer* 1981; **13**:219–224.
5. Gebhart B. Effects of viscous dissipation in natural convection. *Journal of Fluid Mechanics* 1962; **14**: 225–232.
6. Soundalgekar VM, Jaiswal BS, Uplekar AG, Takhar HS. Transient free convection flow of viscous dissipative fluid past a semi-infinite vertical plate. *Applied Mechanics and Engineering* 1999; **4**(2):203–218.
7. Ganesan P, Palani G. Transient free convection flow of a viscous dissipative fluid past a semi-infinite incline plate. *International Journal of Applied Mechanics and Engineering* 2003; **8**(3):395–402.
8. Capper SD, Cash JR, Moore DR. Lobatto–Obrechkoff formulae for 2nd order two-point, boundary value problems. *Journal of Numerical Analysis*, *Industrial and Applied Mathematics* 2006; **1**(1):13–25.

DOI: 10.1002/fld

9. Cash JR, Girdlestone S. Variable step Runge–Kutta Nystrom methods for the numerical solution of reversible systems. *Journal of Numerical Analysis*, *Industrial and Applied Mathematics* 2006; **1**(1):59–80.
10. Iavernaro F, Trigiante D. Discrete conservative vector fields induced by the trapezoidal method. *Journal of Numerical Analysis*, *Industrial and Applied Mathematics* 2006; **1**(1):113–130.
11. Mazzia F, Sestini A, Trigiante D. BS linear multistep methods on non-uniform meshes. *Journal of Numerical Analysis*, *Industrial and Applied Mathematics* 2006; **1**(1):131–144.
12. Carnahan B, Luther HA, Wilkes JO. *Applied Numerical Methods*. Wiley: New York, 1969.

DOI: 10.1002/fld